Toward Remote Sensing of the Net Sea Ice Volume Flux in the Greenland Sea

Spreen, G.[(1)], S. Kern[(1)], R. Ezraty [(2)], H. Witte[(3)], and D. Stammer[(1)]

[(1)]Center for Marine and Atmospheric Sciences, Institute of Oceanography, Bundesstrasse 53, D-20146 Hamburg, Germany, email-address of corresponding author: spreen@ifm.zmaw.de
[(2)]Departement d'Oceanographie Physique et Spatiale, IFREMER Centre de Brest, BP. 70, 29280 Plouzane, France
[(3)]Alfred-Wegener Institute for Polar and Marine Sciences, Bussestrasse 24, D-27570 Bremerhaven, Germany

ABSTRACT

The present paper deals with a multi-sensor approach to improve current knowledge about the net sea-ice volume flux in the Greenland Sea. This approach combines new data from space-borne active and passive microwave, visible/infrared remote sensing with space-borne laser altimeter elevation measurements and ground-based observations of ice thickness and draft. Preliminary results suggest to first focus on the improvement of the conversion of elevation data into sea-ice freeboard which was obtained to vary by up to two meters following a wave-like pattern across the northern entrance of Fram Strait for both, spring and fall, 2003. High-pass filtering in combination with additional data to identify open water areas is used to solve this problem. Next steps, the conversion of freeboard into thickness, calculation of an ice-area flux with enhanced spatial resolution and, finally, ice-volume flux, have been prepared and will require a careful handling of the accuracy and differences in spatial and temporal resolutions of the involved data. Results of this approach will assist analysis, interpretation, and evaluation of CryoSat data, because of similar problems in the conversion of the measured elevation into freeboard and thickness.

1 INTRODUCTION

The sea ice extent of the Arctic Ocean is shrinking as is evident from remote sensing data of the past 30 years [1]. It is expected to further decrease in response to accelerated Arctic Climate warming [2]. Moreover, Arctic sea ice seems to have thinned substantially since the late 1950s [3, 4, 5]. Together, this means a significant reduction of the Arctic sea ice volume. Among others, two main processes can be identified for a decrease in the Arctic sea ice volume: a change in the net amount of sea ice production and the export out of the Arctic Ocean. The first process depends on the length of the freezing period, snow accumulation, and meteorological conditions. The second process is merely determined by the sea ice export through Fram Strait into the Greenland Sea. The export is highly variable, e.g. [6], and its amount is determined by the sea ice thickness at the northern entrance of the Fram Strait and the wind forcing. It was shown by [7] that sea ice export through Fram Strait can occur in surge-like events, where large portions of the old, thick ice leave the Arctic Ocean. Depending on the strength and location of Beaufort Gyre and Transpolar Drift it takes several years until ice of similar thickness has formed again.

While sea ice extent is measured using remote sensing techniques routinely, daily and globally, measuring its thickness on similar scales is still a challenge. A variety of methods has been developed, ranging from visible sensing from aboard ships by recording thickness of ice floes tilted by the ships' hull, over direct thickness measurements by drilling and ground-based electromagnetic (EM) sounding [5] and Upward Looking Sonar (ULS) used from aboard submarine vessels [8] or moorings [8, 9, 10] measuring the ice draft, to air- and space-borne techniques. Here laser profilers [8] or laser altimetry [11], measuring the ice freeboard and/or the ridge/surface roughness distribution, EM sounding, measuring the ice thickness [8, 12], and radar altimetry, measuring the ice freeboard [13], are employed. Techniques to infer the thin-ice thickness from remote sensing data rely on Synthetic Aperture Radar (SAR) [14, 15], infrared and/or passive microwave remote sensing [16]. Radar altimetry has proven to permit a sufficiently large-scale coverage, to be daylight- and weather-independent, and to permit the retrieval over a wide thickness range; it has therefore been further improved and will be used aboard CryoSat [17].

First results using space-borne laser altimetry for sea-ice thickness sensing in the Arctic are encouraging [11]. Key problems are i) contamination by clouds (not relevant for CryoSat), ii) unknown or inaccurate sea surface height, iii) unknown surface roughness, iv) heterogeneous surface within the effective-field-of-view (EFOV), i.e. ice-water mixture, etc.. A stationary sea ice cover over areas much larger than the EFOV is required for sufficient statistics. In order to obtain the ice thickness from the ice freeboard other parameters are required, e.g., snow depth and ice density. Therefore, best results are expected to be obtained in regions with a stationary sea ice cover which permits to average over long/large periods/areas. These conditions are not met in the Fram Strait/Greenland Sea: sea ice is known to drift several kilometers a day, divergence and convergence can continuously change surface roughness, and snow accumulation is very variable.

The Greenland Sea, however, is one of the main areas in the World Oceans where deep convection and formation of dense cold water takes place. These processes are linked to the freshwater input into and the sea ice formation in the

Greenland Sea. Both is in turn a function of the ice export through Fram Strait. Modeled winter salt fluxes in the region of the Greenland Sea Gyre can easily exceed 40-50 kg/m² [18]. This of ample importance for the density distribution of the water masses exiting the Greenland Sea through Denmark Strait and of the water masses to be entrained into the Atlantic water southwest of Svalbard. In order to better understand and quantify processes taking place in the Greenland Sea, this paper aims at giving the starting point for a multi-sensor study of the net sea ice volume flux (and freshwater and salinity budget) in the Greenland Sea involving data from several satellites, ULS, and in-situ measurements. Similar studies were done by [6, 9]. Their estimated sea-ice volume fluxes vary between 2218 km^3/yr (mean 1991-1998) [6] and 2850 km^3/yr (mean 1990 – 1996) [9]. We are aiming to reduce the uncertainties and extend the time series by use of new and higher resolution data.

2 DATA & CONCEPTS TO GET THE SEA ICE VOLUME FLUX

Two major data sources are used: space-borne remote sensing and ULS. The former permit to estimate sea ice concentration, area, extent, motion, type, and freeboard; the latter allow to measure sea ice draft. By combining area and motion the sea-ice area flux can be derived. Ice area times its thickness yields the volume, which in combination with the ice motion gives the sea ice volume flux. So far, space-borne remote sensing of the sea-ice thickness is restricted to thin ice areas [14, 15, 16] or to just a few weeks per year for limited regions using the ICESat laser altimeter [11] – until the launch of CryoSat [17] in 2005. Both, ICESat and CryoSat, measure the sea-ice freeboard and due to this similar data analyzing strategies may be applied, and similar problems may be solved. Our concept is therefore, to use data from ICESat and various other satellite sensors, ULS, and in-situ measurements to develop a method to obtain a first estimate of the sea-ice thickness distribution in the Greenland Sea and, further, of the net sea-ice volume flux in this region by primarily using space-borne remote sensing data. Table 1 at the end of this paragraph gives an overview about the data at hand for our study.

2.1 Sea ice area-flux

We use data acquired by polar orbiting satellites, i.e. Special Sensor Microwave/Imager (SSM/I), Advanced Microwave Scanning Radiometer (AMSR-E), SeaWinds QuikSCAT (a dual pencil-beam scatterometer operating in Ku-Band), Advanced Very High Resolution Radiometer (AVHRR), Envisat Advanced Synthetic Aperture Radar (ASAR) (wide-swath mode), and ICESats' laser altimeter, all of which, except the last one, provide a good to excellent coverage of the Fram Strait/Greenland Sea. SSM/I and AMSR-E data are the basis for sea-ice concentration, area and extent. Comiso-Bootstrap [19, 20] and NASA-Team algorithm [21] ice concentrations are used for a general overview, and to derive the basic ice-area data to estimate the ice-area flux through Fram/ Denmark Straits at 25km x 25km spatial resolution for 1979 until now. The Artist Sea Ice (ASI) algorithm [22] is used to obtain sea-ice concentrations at 12.5km x 12.5km (SSM/I) or 6.25km x 6.25km (AMSR-E) (background in Fig. 3) spatial resolution. The aim is to improve the above-mentioned basic ice-area data regarding spatial resolution (less contamination by land in flux estimates - particularly in the Denmark Strait). Data from microwave radiometry, scatterometry, and/or visible/infrared remote sensing can be combined to get ice motion vectors; those from SSM/I (and its precursor) and AVHRR data [23] or QuikSCAT data [24] have spatial resolution between 25km and 65km. Those from AMSR-E have a finer spatial resolution and will be used together with ASI algorithm ice concentrations to improve the spatial resolution of the sea-ice area flux to 12.5km x 12.5km or better.

2.2 Sea ice thickness

ULS provide us with information about the sea ice draft with respect to the sea surface (open water) above its position – in our case moorings in the Greenland Sea along 75°N and 79°N (Thanks to H. Witte from AWI, and E. Hansen from Norsk Polarinstitutt, NPI) – by measuring the run time of an acoustic signal between the instrument and the sea ice underside. By assuming snow depth and bulk ice density, the ice thickness can be obtained using the equilibrium equation. ULS measurements can be influenced by the beam-width of the instrument, current, temperature and salinity variations in the water, and the homogeneity of the sea ice within the instruments' EFOV [9]. ULS data will be used in comparison with thickness estimates from space-borne sensors for evaluation, to fill data gaps, and to relate the results obtained by ICESat and CryoSat to past measurements. Errors introduced in the conversion from sea-ice draft into sea-ice thickness by unknown snow depth, inaccurate ice density and sea surface level are smaller compared to doing the same with sea-ice freeboard measurements, because 9/10 of the sea ice is below the water surface. Geographical locations and operation periods of ULS used or going to be used are given in Table 1. We suggest in this context to also use ice thickness measured with the helicopter-based EM-Bird of the AWI [12].
Measurements of the laser altimeter aboard ICESat satellite is the second, presently available data source to be used to derive the sea-ice thickness [25]. ICESat was launched in January 2003 and carries only the Geoscience Laser Altimeter System (GLAS). By measuring the run time of a laser pulse at 1064 nm wavelength between the sensor and the surface, and the returned wave form of that pulse the absolute height of the sensor above the surface is obtained for an EFOV of 70 m every 170 m (see [25] for details). To achieve a high accuracy the pulse run time has to be corrected for atmospheric delays and tides. Additionally the satellite carries an Global Positioning System (GPS), and a star-tracker attitude determination system with which its orbit above a reference ellipsoid is determined

with an accuracy of 5 cm. By subtracting the height above the surface measured by the sensor from its height above the reference ellipsoid the mean elevation of the surface in the EFOV is obtained. After atmospheric and tidal corrections the total error budget for a single ICESat elevation measurement comes up to 13.8 cm [25]. By subtracting the measured height from a realistic estimate of the sea surface height, which has to be calculated from the geoid of the Earth and the actual state of atmosphere and ocean, the sea ice freeboard can be obtained.

2.3 Sea ice volume-flux

Once sea-ice area and motion as well as sea-ice thickness are known, the sea-ice volume and the area and volume fluxes can be determined. A compromise has to be found regarding the different error statistics, frequency, and spatial resolution of the different data sets involved: ice area and motion are provided at scales ranging from a few to about 60 kilometers. Sea-ice thickness data are either point measurements (ULS, drilling) or a continuous profile (EM-Bird, EFOV-size: a few meters), are obtained along a discontinuous profile (ICESat, EFOV-size: 70m), or will be obtained continuously along a 15km wide track (CryoSat, EFOV-size: a few 100m). This variety of spatial and also temporal resolutions (revisit times of the same spot are at least 30 days for ICESat and CryoSat) requires a careful consideration of the data statistics.

Table 1: Overview about data at hand for this study.

	Product	Grid-cell size [km]	Time coverage
Ice concen-tration	AMSR-E (ASI, Bootstrap, NT2)	6.25	Jun. 2002 – today
	SSM/I (ASI)	12.5	Jan. 1996 – today
	SSM/I (Bootstrap)	25.0	Oct. 1978 – today
Ice drift	Merged QuikSCAT – SSM/I (IFREMER)	62.5	Dec. 1991 – today (Winter: Oct. – May)
	AMSR-E (IFREMER)	31.25	Jun. 2002 – today (Winter: Oct. – May)
	Polar Pathfinder Sea Ice Motion Vectors (AVHRR, SMMR, SSM/I, Buoys)	25.0	Nov. 1978 – Mar. 2003
Ice thickness	ICESat freeboard		20. Feb. 2003 – 19. Mar. 2003 25. Sep. 2003 – 18. Nov. 2003
	ULS draft (AWI) at positions	75°N/10°W	Aug. 1991 – Dec. 1992 Aug. 1993 – Oct. 1995 Sep. 1999 – Sep. 2002
		79°N/2°W	Aug. 1997 – Oct. 2001
	ULS draft (NPI) at position:	79°N/4°W	Aug. 1990 – 1999

3 RESULTS & DISCUSSION OF WORK IN PROGRESS

3.1 Area Flux

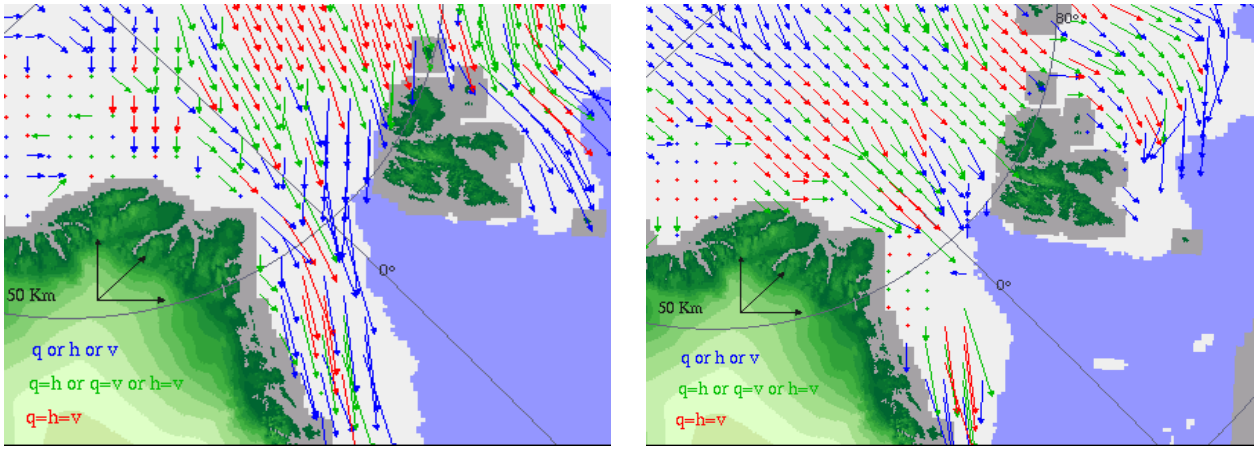

Fig. 1: Ice motion in the Fram Strait derived from combined QuickSCAT (q) and SSM/I horizontal (h) and vertical (v) polarized ice drift vectors [24] for Jan. 13-16, 2003 (left) and Jan. 12-15, 2004 (right). Grid spacing is 62.5 km. Red arrows indicate that three valid, identical ice motion vectors were found and merged; green (blue) arrows indicate two (one) valid ice motion vectors (vector). Arrows show the displacement of the ice within the three days indicated (note arrow scale of 50km); ice mask is the SSM/I ASI algorithm ice concentration.

Using the 85 GHz and 89 GHz channels of the passive microwave radiometers SSM/I and AMSR-E, respectively, increases the spatial resolution of ice concentration, area, and motion from 25 km to 12.5 km and 6.25 km, respectively. Therefore we take ASI algorithm ice concentrations [22] (background of Fig. 2) and the merged QuikSCAT – SSM/I ice motion of the Laboratoire d Océanographie Spatiale, IFREMER/ Centre de Brest (Fig. 1). The accuracy of the used ice motion is very important; 90% of the variance of the ice-volume flux is attributed to variability of the motion field [26]. Therefore, the area flux has to be determined very accurately in order to keep the total error for the volume flux small. Ice area and motion are available from microwave radiometry and visible/ infrared imagery since 1979 (Table 1). However, since we are using newer data, which are derived from measurements of other sensors and/or at a finer spatial resolution, some validation has be done in advance. Moreover, the kind of ice motion data shown in Fig.2 is only available for winter (October to May). In summer, the lost contrast in surface signatures inhibits ice motion retrieval. Other methods or data sources have to be used instead.

3.2 Ice thickness

The height above the surface measured by ICESat can be converted into an estimate of the elevation above the Earths' geoid and/or above the sea surface, which, in sea-ice covered regions can be interpreted as sea-ice freeboard. This can be used to derive the sea-ice thickness assuming constant values of snow depth and bulk ice density. In our study we have done first steps towards obtaining sea-ice freeboard from ICESat elevation measurements. The steps completed, occurred problems and error sources are discussed in the following.

1. The elevation measured by ICESat is the height above a reference ellipsoid and not the height above the sea surface. As a first approach the differences of the ellipsoid to a state-of-the-art geoid were subtracted from the ICESat elevation data. One sample result is shown in Fig. 2. Since approximately 1/10 of the floating ice is above the sea surface, freeboards between 0 and 50 cm can be expected. In Fig. 2 some regions show positive freeboards well above 50cm (red ellipse) while others show negative freeboards (blue ellipses). This freeboard distribution stays almost constant during both periods (spring and fall, Table 1) and can be associated to a) an inaccurate geoid and b) sea surface height anomalies which are not considered. Such anomalies can be caused by wind stress, variations in atmospheric pressure, ocean currents, density anomalies of the seawater and uncorrected tides.
   Therefore other methods have to be used to get a proper geoid and valid sea surface height to be subtracted from the ICESat elevation data to obtain a realistic sea-ice freeboard. One approach is to use the fact that sea surface height anomalies occur on larger scales than the sea-ice freeboard varies within the EFOV. By filtering the elevation data with a high-pass filter it is possible to eliminate the large scale anomalies. In the resulting dataset open water has to be identified either by simply taking the minimum elevations as open water or by using additional data as AMSR-E ASI algorithm ice concentrations (background Fig. 2) to identify open water. Both methods are currently under development.

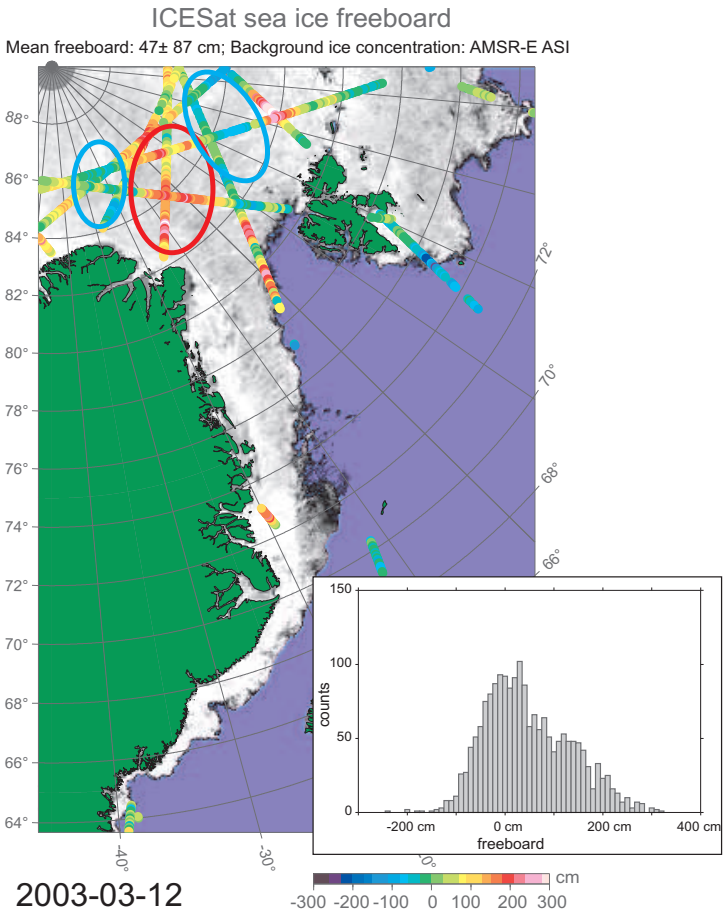

Fig. 3: Sea-ice freeboard calculated by subtracting a state-of-the-art geoid from ICESat elevation measurements (color-coded discs, size not to scale) superposed on a map of the ASI algorithm AMSR-E ice concentration (blue: open water, white 100% ice, medium gray: 50% ice) for March 12, 2003. Ellipses mark regions of pronounced under- or overestimation of the ice freeboard which stay stable for considered periods (see text and Table 1). The insert is the histogram of all ICESat ice freeboards shown.

2. In order to reduce the measurement error and errors introduced by the filtering several measurements have to be averaged to get useful freeboards, e.g., over a period of one week.
3. To obtain an ice-thickness profile across Fram Strait data from several ICESat over-flights are needed.
4. The largest error source for the conversion of sea-ice freeboard into thickness is the unknown snow depth, which can be expected to be quite high in the Fram Strait because of the presence of old ice and the proximity to open water and therefore higher atmospheric water contents as compared to the inner Arctic. Additionally, a large portion of the sea ice is multiyear ice, which in its upper few 10 centimeters has a considerably smaller density than first-year ice (920 kg/m^3). Typical snow densities are around one third of that. In order to derive the ice thickness one has either to know the snow depth or has to adapt the bulk ice density accordingly. Like sea-ice thickness the snow depth on sea ice is difficult to measure from space. For AMSR-E and SSM/I a snow depth algorithm exists [27], which, however, is less accurate for multiyear ice and in the marginal ice zone. Averaging the snow depth over, e.g., one week would reduce uncertainties and make this a useful dataset for our analysis. Other sources of snow depth are climatologies or snow accumulation data provided by a numerical model.

We intend to validate/evaluate the ICESat ice-thickness with data from ULS (see below), data obtained with the helicopter-based EM-Bird (AWI) and from ice-core drilling. Another possibility to get the correct freeboard height is to calibrate the elevation data with SAR data [11]. They identified young ice areas in consecutive RADARSAT-1 SAR images and by matching these to the corresponding ICESat data they obtained locations of zero freeboard. To validate our more general approach a similar study will be carried out, for which about 25 RADARSAT-1 SAR and Envisat ASAR images have been ordered for the first ICESat period (Table 1).

ULS

ICESat ice thickness data only exists since February 2003 and is not recorded continuously (Table 1). In order to evaluate ICESat ice thickness data, to extend the time series into the past and to fill gaps in the ICESat dataset we are using sea-ice draft measurements of moored ULS. Fig. 4 shows the monthly mean ice draft of the AWI moorings at 79° N including measurements of open water together with the standard deviation. Negative values result from the assumption of a Gaussian data distribution which is not correct here but was applied for simplicity. The ice draft is highly variable on a monthly scale (large standard deviations) and also on longer term. The monthly mean draft varies between zero and 2.2 m. A seasonal cycle cannot be identified. For the shown period, the thickest ice was measured in summer 1998, which is due to the release of thick multiyear from north of Greenland through the Fram Strait, whereas zero draft was recorded in March 1999. The latter can be explained by a westward shift of the ice edge as is evident also in Fig. 2. Next step is to convert these data into ice thickness.

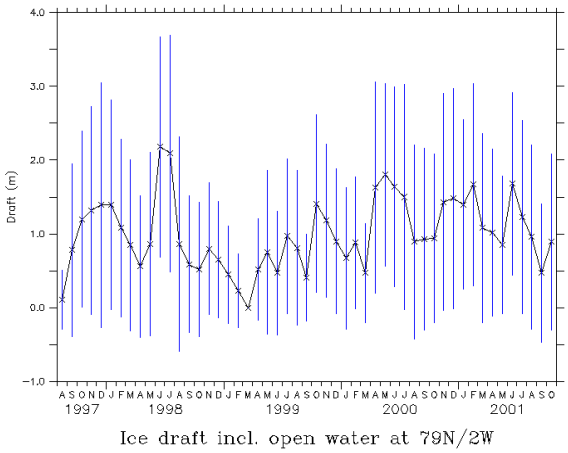

Fig. 4: Monthly mean ice draft plus/minus one standard deviation measured by ULS from AWI moored in the Fram Strait at 79°N.

In order to get a representative profile of the ice thickness across Fram Strait as is needed to estimate the ice volume flux such ULS ice-thickness data have to be extrapolated across the Fram Strait (see [6,9]). By using ICESat, and, in the near future, CryoSat data the extrapolation can be replaced by an interpolation and a much more representative ice thickness profile across Fram Strait can be expected.

4 SUMMARY & OUTLOOK

A multi-sensor strategy to obtain the sea-ice volume flux in the Greenland Sea is presented. The aim is to extend the findings of [6, 9] by adding new ice thickness data derived from ICESat laser altimeter (launched 2003) and CryoSat radar altimeter (to be launched 2005), and ice motion data from microwave radiometry and scatterometry at improved spatial resolution. Among satellite data our approach includes data from moored Upward Looking Sonar (ULS), helicopter-based electromagnetic ice-thickness sounding (EM-Bird) and ice-core drilling. First results reveal that conversion of ICESat elevation measurements into sea-ice freeboard and, further, into thickness requires to solve a couple of problems and shortcomings among which are: 1) Inaccurate sea surface height and/or geoid of the Earth cause almost stationary, unrealistic freeboard variations of up to 2 m in the northern entrance of the Fram Strait. 2) Evaluation data (ULS, EM-Bird) as well as ICESat data have a sparse coverage limiting direct inter-comparisons. 3) ICESat data have to be averaged over a certain period, e.g., one week, and a sufficiently large area to allow a meaningful combination with ice-area and motion data; this is problematic in the Fram Strait/Greenland Sea due to high drift speeds. 4) Conversion of freeboard into thickness requires snow depth and multiyear-ice fraction.

An approach to solve 1) is in progress. Regarding 2) evaluation will be optimized by acquiring as many in-situ, ULS, and EM-Bird data as possible to allow more direct inter-comparison and usage of interpolation instead of extrapolation. Regarding 3) the limited availability of ICESat data itself is a constraint which cannot be changed. Regarding 4) ice classification by means of scatterometry and/or SAR will help to estimate the multiyear-ice fraction and weekly snow depth on sea ice will be estimated from SSM/I and AMSR-E data. If these problems are all solved, ICESat elevation measurements are a comprehensive dataset for sea ice thickness. Compared to current alternatives, it has the highest spatial and, during its periods of operation, also temporal coverage. In combination with an improved ice-area flux the knowledge about Greenland Sea ice-volume flux can be substantially improved.
The CryoSat mission addresses as well the lack of knowledge about sea-ice thickness and volume, and aims at solving it also by measuring the sea-ice freeboard. Therefore, it can be expected that similar problems will arise, particularly in the conversion of the elevation measurements into sea-ice freeboard (sea surface height and geoid uncertainties, a heterogeneous surface within sensors' field-of-view) and, further, into thickness (unknown snow depth and ice density). We believe that the results of our study will assist analysis, interpretation and evaluation of CryoSat measurements. As a future step the obtained ice-volume fluxes can be assimilated into coupled ice-ocean models which would allow to extend the time-series further into the past, to relate the fluxes to processes in the Greenland Sea, and to predict the impact of an accelerated decay of the Arctic sea ice cover.

5 ACKNOWLEDGEMENTS

The authors acknowledge provision of ICESat data and AMSR-E data by the National Snow and Ice Data Center (NSIDC), Boulder, CO, USA.

6 REFERENCES

1. Cavalieri D. J., et al., 30-Year satellite record reveals contrasting Arctic and Antarctic decadal sea ice variability, *Geophys. Res. Lett.*, 30(18), 1970, doi:10.1029/2003GL018031, 2003.
2. Johannesson O. M., et al., Arctic climate change: observed and modeled temperature and sea-ice variability, *Tellus*, 56A(4), 328-341, 2004.
3. Rothrock D. A., et al., Thinning of the Arctic sea-ice cover, *Geophys. Res. Lett.*, 26(23), 3469-3472, 1999.
4. Rothrock D. A., et al., The Arctic ice thickness anomaly of the 1990s: A consistent view from observations and models, *J. Geophys. Res.*, 108, doi:10.1029/2001JC001208, 2003.
5. Haas C., Late-summer sea ice thickness variability in the Arctic Transpolar Drift 1991-2001 derived from ground-based electromagnetic sounding, *Geophys. Res. Lett.*, 31, L09402, doi:10.1029/2003GL019394, 2004.
6. Kwok R., et al., Fram Strait sea ice outflow, *J. Geophys. Res.*, 109, C01009, doi:10.1029/2003JC001785, 2004.
7. Pfirman S., et al., Variability in Arctic sea ice drift, *Geophys. Res. Lett.*, 31, L16402, doi:10.1029/ 2004GL020063, 2004.
8. Wadhams P., *Ice in the Ocean*, Gordon and Breach Science Publishers, London, 351pp., 2002.
9. Vinje T., et al., Monitoring ice thickness in the Fram Strait, *J. Geophys. Res.*, 103(C10), 10,437-10,449, 1998.
10. Widell K., et al., Sea ice velocity in the Fram Strait monitored by moored intruments, *Geophys. Res. Lett.*, 30(19), 1982, doi:10.1029/ 2003GL018119, 2003.
11. Kwok R., et al., ICESat observations of Arctic sea ice: A first look, *Geophys. Res. Lett.*, 31, L16401, doi:10.1029/2004GL020309, 2004.
12. Haas C., Airborne EM Sea-ice thickness profiling over brackish Baltic Sea water, *Proc. Int. Symp. on Ice, St. Petersburg, Russia, June 19-23, 2004.*
13. Laxon S., et al., High interannual variability of sea ice thickness in the Arctic region, *Nature*, 425, 947-950, 2003.
14. Wadhams P., et al., SAR imaging of wave dispersion in Antarctic pancake ice and its use in measuring ice thickness, *Geophys. Res. Lett.*, 31, L15305, doi:10.1029/ 2004GL020340, 2003.
15. Yu Y. and Lindsay R., Comparison of thin ice thickness distributions derived from RADARSAT Geophysical Processor System and advanced very high resolution radiometer data sets, *J. Geophys. Res.*, 108(C12), 3387, doi:10.1029/2002JC001319, 2003.
16. Martin S., et al., Estimation of the thin ice thickness and heat flux for the Chukchi Sea Alaskan coast polynya from Special Sensor Microwave/Imager data, 1990-2001, *J. Geophys. Res.*, 109, C10012, doi:10.1029/ 2004JC002428, 2004.
17. ESA-ESTEC, CryoSat : Mission and Data Description, CS-RP-ESA-SY-0059, Dec. 15, 2003.
18. Pedersen L. T. and Coon M. D., A sea ice model for the marginal ice zone with an application to the Greenland Sea, *J. Geophys. Res.*, 109, C03008, doi:10.1029/2003JC001827, 2004.
19. Comiso J. C., SSM/I concentrations using the Bootstrap Algorithm, NASA Report RP 1380, 40pp., 1995.
20. Comiso J., Bootstrap sea ice concentrations from NIMBUS-7 SMMR and DMSP SSM/I, Boulder, CO, USA, National Snow and Ice Data Centre, Digital Media, 1999, updated 2003.
21. Cavalieri D. J., et al., Aircraft active and passive microwave validation of the sea ice concentration from the Defense Meteorological Satellite Program Special Sensor Microwave/Imager, *J. Geophys. Res.*, 96, 21,998-22,008, 1991.
22. Kaleschke L., et al., SSM/I sea ice remote sensing for mesoscale ocean-atmosphere interaction analysis, *Can. J. Rem. Sens.*, 27(5), 526-537, 2001.
23. Fowler C., Polar Pathfinder Daily 25km EASE-Grid Sea Ice Motion Vectors, Boulder, CO, USA, National Snow and Ice Data Centre, Digital Media, 2003.
24. Ezraty R. and Piollé J.-F., Sea ice drift in the central arctic combining QuikScat and SSM/I sea ice drift data, User's Manual, Version 1.0, Brest, France, IFREMER, ftp://ftp.ifremer.fr/ifremer/cersat/products/gridded/psi-drift/documentation/merged.pdf, Apr 2004.
25. Zwally H. J., et al., ICESat's laser measurements of polar ice, atmosphere, ocean, and land, *J. Geodyn*, Vol. 24, 405-445, 2002.
26. Thomas D., et al., Assimilating satellite concentration data into an Arctic sea ice mass balance model, 1979-1985, *J. Geophys. Res.*, 101, 20,849-20,869, 1996.
27. Markus T. and Cavalieri D. J., Snow depth distribution over sea ice in the Southern Ocean from satellite passive microwave data, Antarctic Sea Ice: Physical Processes, Interactions and Variability, Antarctic Research Series, Vol. 74, pp 19-39, American Geophysical Union, Washington, DC, 1998.